南京航空航天大学

论 文 集

（二〇〇九年） 第30册

材料科学与技术学院

（第2分册）

南京航空航天大学科技部编

二〇一〇年五月

材料科学与技术学院

二

材料科学与技术学院

061 系

062 系

063 系

序号	姓 名	职 称	单 位	论 文 题 目	刊物.会议名称	年、卷、期	类别
79	钟 杰 郑 勇 袁 泉 张一欣 余立新	硕士 教授 硕士 硕士 高工	061 061 061 061 外单位	Fabrication of functionally graded Ti(C, N)-based cermets by double-glow plasma carburization	Int. Journal of Refractory Metals & Hard Materials	2009.27.3	
80	袁 泉 郑 勇 于海军	硕士 教授 硕士	061 061 061	Synthesis of nanocrystalline Ti(C,N) powders by mechanical alloying and influence of alloying elements on the reaction	Int. Journal of Refractory Metals & Hard Materials	2009.27.1	
81	袁 泉 郑 勇 于海军	硕士 教授 硕士	061 061 061	Mechanism of synthesizing nanocrystalline TiC in different milling atmospheres	Int. Journal of Refractory Metals & Hard Materials	2009.27.4	
82	庞旭明 郑 勇 王少刚 王秋红	硕士 教授 副教授 硕士	061 061 061 061	Effect of Mn on valence –electron structure and properties of hard phase in Mo2FeB2-based cermets	Int. Journal of Refractory Metals & Hard Materials	2009.27.4	
83	张一欣 郑 勇 钟 杰 袁 泉 吴 鹏	硕士 教授 硕士 硕士 硕士	061 061 061 061 061	Effect of carbon content and cooling mode on the microstructure and properties of Ti(C,N)-based cermets	Int. Journal of Refractory Metals & Hard Materials	2009.27.6	
84	郑建智 承 新 郑 勇 严永林 赵能伟	硕士 硕士 教授 硕士 硕士	061 061 061 061 061	烧结工艺和碳加入量对 Mo_2FeB_2 基金属陶瓷显微组织和性能的影响	机械工程材料	2009.33.3	
85	郑建智 郑 勇 庞旭明 承 新 江赛华 林新刚	硕士 教授 硕士 硕士 学士 学士	061 061 061 061 061 061	Mo_2FeB_2 基金属陶瓷烧结过程中显微组织和力学性能的变化	硬质合金	2009.26.2	
86	钟 杰 郑 勇 张一欣	硕士 教授 硕士	061 061 061	功能梯度 Ti(C, N)基金属陶瓷制备技术	复合材料学报	2009.26.3	
87	张一欣 郑 勇 郑建智 赵永乐	硕士 教授 硕士 硕士	061 061 061 061	冷却方式对 Ti(C,N)基金属陶瓷显微组织和力学性能的影响	硬质合金	2009.26.1	

序号	姓名	职称	单位	论文题目	刊物.会议名称	年、卷、期	类别
88	钟 杰 郑 勇 严永林 庞旭明	硕士 教授 硕士 硕士	061 061 061 061	功能梯度硬质合金与金属陶瓷制备技术的研究进展	机械工程材料	2009.33.2	
89	庞旭明 郑 勇 王少刚 王秋红	硕士 教授 副教授 硕士	061 061 061 061	Mn 对 Mo_2FeB_2 基金属陶瓷组织和力学性能的影响	中国有色金属学报	2009.19.9	
90	王 慧 薛松柏 陈文学	博士 正高 硕士	061 061 061	Effects of Ga-Ag, Ga-Al and Al-Ag additions on the wetting Characteristics of Sn-9Zn-X-Y lead-free solders	Journal of Materials Science: Materials in Electronics	2009. 20.12	
91	王 慧 薛松柏 陈文学	博士 正高 硕士	061 061 061	Effects of Ga, Al, Ag, and Ce multi-additions on the wetting characteristics of Sn-9Zn lead-free solder	Rare Metals	2009.28.6	
92	张 亮 薛松柏 皋利利 曾 广 盛 重 陈 燕	博士 正高 博士 硕士 硕士 工程师	061 061 061 061 061 外单位	Effects of rare earths on properties and microstructures of lead-free solder alloys	Journal of Materials Science: Materials in Electronics	2009. 20.8	
93	张 亮 薛松柏 皋利利 陈 燕 禹胜林 盛 重 曾 广	博士 正高 博士 工程师 正高 硕士 硕士	061 061 061 外单位 061 061 061	Effects of trace amount addition of rare earth on properties and microstructureof Sn-Ag-Cu alloys	Journal of Materials Science: Materials in Electronics	2009.20.12	
94	张 亮 薛松柏 皋利利 曾 广 盛 重 陈 燕	博士 正高 博士 硕士 硕士 工程师	061 061 061 061 061 外单位	Determination of Anand parameters for SnAgCuCe solder	Modelling and Simulation in Materials Science and Engineering	2009.17.7	
95	张 亮 薛松柏 陈 燕 韩宗杰 王俭辛 禹胜林 卢方焱	博士 正高 工程师 博士 博士 正高 硕士	061 061 外单位 061 061 061 061	Effects of cerium on Sn-Ag-Cu alloys based on finite element simulation and experiments	Journal of Rare Earths	2009.27.1	

序号	姓名	职称	单位	论文题目	刊物.会议名称	年、卷、期	类别
96	韩宗杰 薛松柏 王俭辛 张　昕 禹胜林 张　亮	博士 正高 博士 硕士 博士 博士	061 061 061 061 061 061	Laser Soldering of Fine Pitch QFP Devices Using Lead-Free Solders	Journal of electronic packaging	2009.131.2	
97	王俭辛 薛松柏 韩宗杰 禹胜林 陈　燕 史益平 王　慧	博士 正高 博士 博士 工程师 硕士 博士	061 061 061 061 外单位 061 061	Effects of rare earth Ce on microstructures, solderability of Sn-Ag-Cu and Sn-Cu-Ni solders as well as mechanical properties of soldered joints	Journal of alloys and compounds	2009.467.1-2	
98	王　慧 薛松柏 陈文学	博士 正高 硕士	061 061 061	Ga、Al 对 Sn-Zn 钎料耐蚀及高温抗氧化性能的影响	稀有金属材料与工程	2009.38.12	
99	陈文学 薛松柏 王　慧 王俭辛 韩宗杰	硕士 正高 博士 博士 博士	061 061 061 061 061	Solderability and intermetallic compounds formation of Sn-9Zn-xAg lead-free solders wetted on Cu substrate	Rare Metals	2009.28.6	
100	赖忠民 薛松柏 卢方焱 顾立勇 顾文华	博士 博士 博士 工程师 高工	061 061 061 外单位 外单位	Effects of Ga and In on the properties of AgCuZn cadmium-free filler metal	China Welding	2009.18.4	
101	王　慧 薛松柏 陈文学	博士 正高 硕士	061 061 061	Effects of Al, Ga, and Ag on the surface properties and wetting reactions of Sn-9Zn-X solders	China Welding	2009. 18.2	
102	肖正香 薛松柏 金春玉 张　亮 皋利利	硕士 正高 硕士 博士 博士	061 061 外单位 061 061	CuCGA 器件焊点热疲劳行为数值模拟	焊接学报	2009.30.12	
103	叶　焕 薛松柏 张　亮 王　慧	硕士 正高 博士 博士	061 061 061 061	CSP 器件无铅焊点可靠性的有限元分析	焊接学报	2009.30.11	
104	盛　重 薛松柏 张　亮 皋利利	硕士 正高 博士 博士	061 061 061 061	QFP 器件微焊点可靠性分析	焊接学报	2009.30.10	

序号	姓名	职称	单位	论文题目	刊物.会议名称	年、卷、期	类别
105	朱　宏 薛松柏 盛　重	博士 正高 硕士	061 061 061	合金元素对 6063 铝合金阶梯焊中温钎料性能的影响	焊接学报	2009. 30.8	
106	盛　重 薛松柏 张　亮 皋利利	硕士 正高 博士 博士	061 061 061 061	QFP 器件微焊点热疲劳行为分析	焊接学报	2009.30.12	
107	朱　宏 薛松柏 盛　重	博士 正高 硕士	061 061 061	6063 铝合金氧化膜与 CsF-AlF3 及 KF-AlF3 钎剂的反应机制	焊接学报	2009. 30.9	
108	朱　宏 薛松柏 盛　重	博士 正高 硕士	061 061 061	6063 铝合金阶梯焊中温钎料腐蚀性能分析	焊接学报	2009.30.10	
109	戴　玮 薛松柏 张　亮 盛　重	硕士 正高 博士 硕士	061 061 061 061	不同阵列 PBGA 器件焊点可靠性分析	焊接学报	2009.30.9	
110	戴　玮 薛松柏 张　亮 姬　峰	硕士 正高 博士 硕士	061 061 061 061	基于田口法的 PBGA 器件焊点可靠性分析	焊接学报	2009.30.11	
111	王　慧 薛松柏 陈文学	博士 正高 硕士	061 061 061	复合添加 Ga、Al、Ag 对 Sn-9Zn 钎料性能的影响	焊接学报	2009.30.6	
112	王　慧 薛松柏 陈文学 王检辛	博士 正高 硕士 博士	061 061 061 061	不同钎剂对 Sn-Zn 系无铅钎料润湿特性的影响	焊接学报	2009. 30.1	
113	胡玉华 薛松柏 陈文学 王　慧	硕士 正高 硕士 博士	061 061 061 061	Sn-9Zn-xAg 钎料在 Cu 基材上润湿性能及界面组织的研究	材料工程	2009.6	
114	张　亮 薛松柏 卢方焱 韩宗杰 禹胜林	博士 正高 硕士 博士 博士	061 061 061 061 061	基于蠕变模型细间距器件焊点疲劳寿命预测	机械工程学报	2009. 45.94	
115	张　亮 薛松柏 曾　广 皋利利 陈　燕	博士 正高 硕士 博士 工程师	061 061 061 061 外单位	铈对 SnAgCu 钎料的显微组织和性能影响	中国稀土学报	2009. 27.2	

序号	姓 名	职 称	单 位	论 文 题 目	刊物.会议名称	年、卷、期	类别
116	陈文学 薛松柏 王 慧 王俭辛	硕士 正高 博士 博士	061 061 061 061	Sn-9Zn-xAg 无铅钎料润湿性能及焊点力学性能	焊接学报	2009.30.6	
117	卢方焱 薛松柏 张 亮 赖忠民 顾立勇 顾文华	硕士 正高 博士 博士 工程师 高工	061 061 061 061 外单位 外单位	镓对 AgCuZn 钎料组织和性能的影响	焊接学报	2009. 30.1	
118	姬 峰 薛松柏 张 亮 王 慧	硕士 正高 博士 博士	061 061 061 061	QFN 封装焊点可靠性的有限元分析	焊接学报	2009.30.10	
119	薛松柏 张 亮 皋利利 韩宗杰 禹胜林 朱 宏	正高 博士 博士 博士 博士 博士	061 061 061 061 061 061	航空器制造中的焊接技术	航空制造技术	2009.17	
120	肖正香 薛松柏 张 亮 皋利利	硕士 正高 博士 博士	061 061 061 061	微量元素对 Sn-Zn 系钎料性能和组织的影响	电焊机	2009.39.11	
121	叶 焕 薛松柏 张 亮 皋利利 曾 广	硕士 正高 博士 博士 硕士	061 061 061 061 061	稀土元素对 SnAgCu 钎料性能的影响	电焊机	2009.39.10	
122	王 慧 薛松柏 陈文学 胡玉华	博士 正高 硕士 硕士	061 061 061 061	Ag 对 Sn-9Zn 无铅钎料耐蚀性能影响的研究	焊接	2009. 增刊 1	
123	皋利利 薛松柏 张 亮 盛 重	博士 正高 博士 硕士	061 061 061 061	微量元素对 Sn-Ag-Cu 系钎料以及焊点的影响	焊接	2009. 增刊 1	
124	薛松柏 王 慧 陈文学 顾立勇 顾文华	正高 博士 硕士 工程师 高工	061 061 061 外单位 外单位	Sn-Zn 系无铅钎料研究中的几个热点	第十七届全国钎焊及特种连接技术交流会议		

序号	姓名	职称	单位	论文题目	刊物.会议名称	年、卷、期	类别
125	赖忠民 张　亮 薛松柏 卢方焱	博士 博士 正高 硕士	061 061 061 061	合金元素对 Ag-Cu-Zn 系钎料影响的研究现状及发展趋势	第十七届全国钎焊及特种连接技术交流会议		
126	张　满 薛松柏 王　慧	博士 正高 博士	061 061 061	锌基中温铝钎料的研究现状及发展趋势	第十七届全国钎焊及特种连接技术交流会议		
127	马　骋 薛松柏 吴铭方 陈　健	博士 正高	061 061 外单位 外单位	Ti(C,N)基金属陶瓷与 45 号钢真空钎焊研究	第十七届全国钎焊及特种连接技术交流会议		
128	薛松柏 张　亮 盛　重 皋利利	正高 博士 硕士 博士	061 061 061 061	微电子组装焊点可靠性研究进展	焊接	2009. 增刊 1	
129	李　勇 肖　军 谭永刚 原永虎	副教授 教授 硕士 硕士	061 061 061 061	BMI-QC130 双马树脂拉挤工艺	复合材料学报	2009.26.5	
130	李　勇 肖　军 谭永刚 原永虎 党旭丹	副教授 教授 硕士 硕士 博士	061 061 061 061 061	X-cor 夹层结构压缩性能研究	航空学报	2009.30.3	
131	罗海燕 李　勇 肖　军 还大军	硕士 副教授 教授 博士	061 061 061 061	复合材料自动辅带技术研究——曲面辅带轨迹算法	航空学报	2009.30.9	
132	叶　进 文立伟 李　勇 肖　军	硕士 副教授 副教授 教授	061 061 061 061	复合材料自动辅带技术——曲面辅带 CAM 技术	宇航材料工艺	2009.0.4	
133	李　勇 黄炳辉 殷　凯	副教授 研究员 助工	061 机关 机关	完善工程训练体系 培养高素质人才	实验室研究与探索	2009.28.5	
134	唐正霞 沈鸿烈 黄海宾 鲁林峰 尹玉刚 蔡　红	博士 教授 博士 博士 博士 博士	061 061 061 061 061 061	Preparation of high quality polycrystalline silicon thin films by aluminum-induced crystallization	Thin Solid Films	2009.517.19	

序号	姓名	职称	单位	论文题目	刊物.会议名称	年、卷、期	类别
135	唐正霞 沈鸿烈 鲁林峰 江　丰 郭　艳 沈剑沧	博士 教授 博士 博士 硕士 工程师	061 061 061 061 061 外单位	Polycrystalline silicon thin film prepared by aluminum-induced crystallization with native silicon oxide at the aluminum and silicon interface	Journal of Optoelectronics and Advanced Materials	2009.11.8	
136	李　丹 沈鸿烈 鲁林峰 黄海宾 李斌斌	硕士 教授 博士 博士 副教授	061 061 061 061 061	电沉积法制备 ZnO 薄膜的结构与光电性能研究	压电与声光	2009.31.3	
137	蔡　红 沈鸿烈 尹玉刚 鲁林峰 沈剑沧 唐正霞	博士 教授 硕士 博士 工程师 博士	061 061 061 061 外单位 061	The effects of porous silicon on the crystalline properties of ZnO thin films	Journal of Physics and Chemistry of Solids	2009.70.6	
138	黄海宾 沈鸿烈 张　磊 吴天如 鲁林峰 唐正霞 沈剑沧	博士 教授 博士 博士 博士 博士 工程师	061 061 061 061 061 061 外单位	Effects of hydrogen dilution ratio on properties of Boron-doped germanium films by hot-wire Chemical vapor deposition	Journal of Optoelectronics and Advanced Materials	2009.11.11	
139	唐正霞 沈鸿烈 黄海宾 鲁林峰 蔡　红 沈剑沧	博士 教授 博士 博士 博士 工程师	061 061 061 061 061 外单位	Fractal growth of amorphous silicon crystallization induced by aluminum	Journal of Optoelectronics and Advanced Material	2009.11.11	
140	徐　江 卓城之 陶　杰 蒋书运 刘林林	教授 硕士 教授 教授 硕士	061 061 061 外单位 061	Improving the corrosion wear resistance of AISI 316L stainless steel by particulate reinforced Ni matrix composite alloying layer	Journal of Physics D: applied physic	2009.42	
141	徐　江 卓城之 韩德忠 陶　杰 刘林林 蒋书运	教授 硕士 中级 教授 硕士 教授	061 061 外单位 061 061 外单位	Erosion–corrosion behavior of nano-particle-reinforced Ni matrix composite alloying layer by duplex surface treatment in aqueous slurry environment	Corrosion Science	2009.51.5	

序号	姓名	职称	单位	论文题目	刊物.会议名称	年、卷、期	类别
142	徐 江 卓城之 蒋书运	教授 硕士 教授	061 061 外单位	纳米颗粒对 Ni 基复合镀渗层耐冲蚀性能的影响	物理化学学报	2009.25.10	
143	徐 江	教授	061	Investigation on the Behaviour of Sputter-Deposited Nanocrystalline Cr_3Si Film by Double Cathode Glow Discharge	Current Nanoscience	2009.5.4	
144	徐 江 陈哲源 陶 杰 蒋书运 刘子利 徐 重	教授 硕士 教授 教授 副教授 教授	061 061 061 外单位 061 0061	Corrosion behavior of amorphous/nanocrystalline Al-Cr-Fe film deposited by double glow plasmas technique	Science in China Series E: Technological Sciences	2009.52.2	
145	徐 江 孙 建 蒋书运	教授 硕士 教授	061 061 外单位	Mechanical properties of sputter-deposited nanocrystalline Cr_3Si film	Materials Letters	2009.63.12	
146	卓城之 鲁小林 韩德忠 徐 江 刘林林	硕士 初级 中级 教授 硕士	061 理学院 外单位 061 061	纳米 A1203 颗粒增强 Ni 基复合镀渗合金层的腐蚀磨损性能研究	南京大学学报	2009.45.2	
147	杨宗辉 沈以赴 柳秉毅 罗嘉欣	博士 教授 硕士 硕士	061 061 061 061	基于虚拟仪器的焊接热循环测试系统	微计算机信息	2009.25.5-1	
148	于秀平 沈以赴 顾冬冬	硕士 教授 副教授	061 061 061	激光烧结法制备原位增强型多孔镍基复合材料	稀有金属与硬质合金	2009.37.4	
149	连绵炎 沈以赴 顾冬冬	硕士 教授 副教授	061 061 061	机械高能球磨法制备表面多孔金属铝	金属功能材料	2009.16.01	
150	黄 真 沈以赴	硕士 教授	061 061	稀土对机械合金化制备碳钢表面铬合金层的影响	钢铁研究学报	2009.21.7	
151	周娟娟 姚正军	硕士 教授	061 061	POE 增韧改性回收 PP 的注塑成型工艺及其性能	机械工程材料	2009.33.10	
152	杨和梅 姚正军	硕士 教授	061 061	氩氧比例对 Al_2O_3 薄膜结构性能的影响	有色金属	2009.61.3	
153	朱晓林 姚正军	硕士 教授	061 061	Microstructure and corrosion resistance of Fe-Al intermetallic coating on 45 steel synthesized by double glow plasma surface alloying technology	Transactions of Nonferrous Metals Society of China	2009.19.1	

序号	姓 名	职 称	单 位	论 文 题 目	刊物.会议名称	年、卷、期	类别
154	朱晓林 姚正军	硕士 教授	061 061	Q235 钢双汇镍铬共渗层的组织结构和乃是性能	南京大学学报（自然科学版）	2009.45.2	
155	周金堂 姚正军	硕士 教授	061 061	回收 PP 增韧性能的初步探索	材料科学与工程学报	2009.27.2	
156	孟召辉 姚正军	硕士 教授	061 061	聚丙烯的共混改性研究	气和工艺与材料	2009.11	

2.2

Int. Journal of Refractory Metals & Hard Materials 27 (2009) 642–646

Contents lists available at ScienceDirect

Int. Journal of Refractory Metals & Hard Materials

journal homepage: www.elsevier.com/locate/IJRMHM

Fabrication of functionally graded Ti(C, N)-based cermets by double-glow plasma carburization

Zhong Jie [a], Zheng Yong [a,*], Yuan Quan [a], Zhang Yixin [a], Yu Lixin [b]

[a] College of Material Science and Technology, Nanjing University of Aeronautics and Astronautics, Nanjing 210016, China
[b] Suzhou Kingdream Shareate Cemented Carbide Co. Ltd., Suzhou 215121, China

ARTICLE INFO

Article history:
Received 21 July 2008
Accepted 16 October 2008

Keywords:
Functionally graded cermet
Double-glow plasma carburization
Microstructure
Forming mechanism

ABSTRACT

Functionally graded Ti(C, N)-based cermets were prepared via vacuum liquid sintering and subsequent double-glow plasma carburization. The microstructure was characterized using scanning electron microscope (SEM), electron probe microanalysis (EPMA) and X-ray diffraction (XRD). It was found that a surface zone enriched in titanium, molybdenum, tungsten, carbon and nitrogen, deficient in nickel was introduced by double-glow plasma carburization. The high carbon activity in the surface region drove titanium, molybdenum and tungsten elements inside the substrate to diffuse outwards, consequently the nickel-rich binder was forced to transport inwards. The formation of the binder-deficient layer was controlled by the diffusion of the alloy elements and the growing rate did not follow the parabolic law.

1. Introduction

Ti(C, N)-based cermets are used as cutting tools for the high hardness, good thermal stability, excellent creep and wear resistance [1,2], but the appreciably low strength restricts their use. This issue could be commendably solved by introducing graded structure into the materials [3].

Over the past years, many approaches were suggested to prepare functionally graded hardmetals and cermets, such as coating and heat-treatment in nitrogen [4,5]. Coating could greatly enhance the surface wear resistance by depositing a layer of hard material on the tough bulk [6]. Since the coating process is usually carried out at high temperature, cracks are formed ineluctably due to different thermal expansion coefficients between coatings and substrate [7]. During machining, the cracks propagated through the entire coating and resulted in catastrophic failure. These cracks could be avoided by heat-treatment in nitrogen [8]. However, due to tiny solubility of nitrogen in the nickel binder, the gradient layer was limited, although a long heat-treatment time was applied [3].

It was found that the formation of the graded structure resulted from the differences of the affinity between nitrogen and different alloy elements during nitriding [9]. As there is also a remarkable difference of the affinity between carbon and these metallic elements, a gradient is also anticipated by carburization. However there is no report on the issue till now.

The double-glow plasma surface alloying technology (known as Xu-Tec process or DG technology) was developed in 1980, and had been successfully used in surface modification of metal materials [10]. The Xu-Tec process is a unique and hybrid technique using a double-glow discharge phenomenon inside a vacuum chamber, which has evolved from both plasma nitriding and sputtering techniques [11]. In general, any metallic or metalloid element could be alloyed into the surface of the conductive substrates. In the present study, functionally graded Ti(C, N)-based cermets were prepared via vacuum liquid sintering and subsequent double-glow plasma carburization. Then the microstructure and composition distribution of the carburized cermets were investigated. In addition, the forming mechanism of the graded layer was also discussed.

2. Experimental procedure

The schematic presentation of double-glow plasma surface alloying equipment is shown in Fig. 1. There are three electrodes in the vacuum chamber of the double-glow plasma surface alloying apparatus: one anode and two negatively charged members [12]. The negatively charged members include cathode (workpiece) and the source electrode.

In the present experiment, the source electrode was made up of carbon. The cathode and source electrode were surrounded by glow discharge, one glow discharge heated the substrate to be alloyed and the second glow struck the source electrode [11], which was known as double-glow discharge. During carburization, the cermets were heated to a designed temperature by plasma bombardment and carbon was sputtered by the second glow from

* Corresponding author. Tel.: +86 25 84236039; fax: +86 25 52112626.
E-mail address: yzheng_only@263.net (Z. Yong).

0263-4368/$ - see front matter © 2008 Elsevier Ltd. All rights reserved.
doi:10.1016/j.ijrmhm.2008.10.013

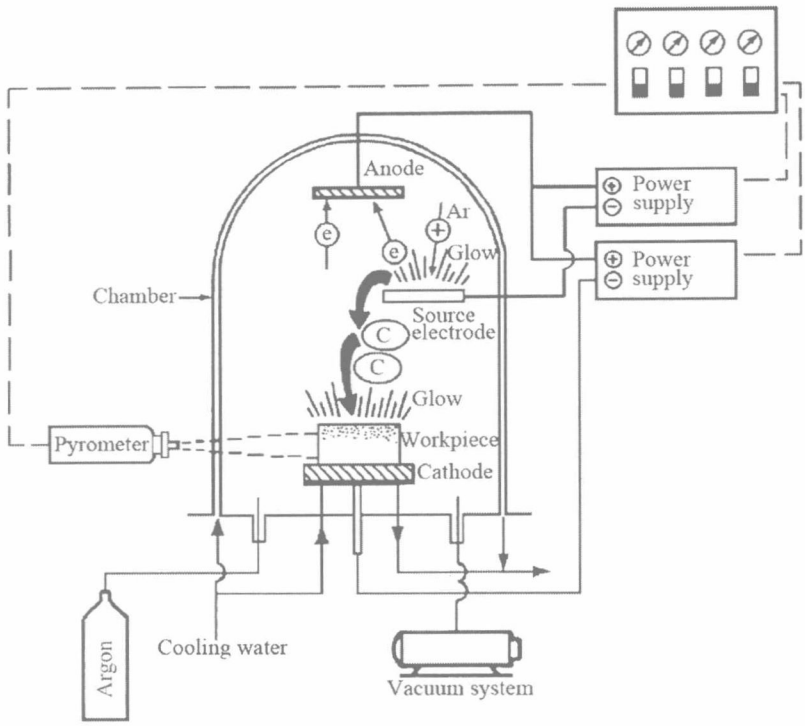

Fig. 1. Sketch map of equipment for double-glow plasma carburization [11].

Table 1
Chemical composition and mean particle size of initial powders.

Powders	Particle size (μm)	Chemical composition (wt.%)
TiC (after milled for 24 h)	0.51	O ⩽ 1.21
TiN (after milled for 24 h)	0.52	O ⩽ 1.10
WC	0.85	C_{free} ⩽ 0.025, O ⩽ 0.21
Ni	1.70	C_{free} ⩽ 0.03, O < 0.22
Mo	2.60	C_{free} ⩽ 0.0012, O ⩽ 0.10

the source electrode, then flied towards and subsequently diffused into the substrate surface to form a gradient layer.

The characteristics of the initial powders are summarized in Table 1. The compositions of the two kinds of cermets with different nickel content considered in the present study are TiC-10 wt.% TiN-21 wt.% Ni-16 wt.% Mo-8.4 wt.% WC and TiC-10 wt.% TiN-32 wt.% Ni-16 wt.% Mo-8.4 wt.% WC, respectively.

The powder mixtures were ball milled in alcohol for 24 h, the mass ratio of ball to material was 7:1 and the rotational speed was 260 rpm. The bar specimens with a dimension of 40.0 mm × 8.0 mm × 6.5 mm were dry pressed and then sintered in vacuum at 1430 °C for 1 h. The as-sintered specimens were polished and carburized at 1100 °C and 1200 °C. At each temperature, different samples were carburized for 90 min, 120 min, 150 min and 180 min, respectively. The discharged gas was pure argon.

The microstructures of the as-sintered as well as carburized material were observed by scanning electron microscope operated at 20 kV (SEM QVANTA200, FEI) in backscattered-electron (BSE) mode. Compositional depth profiles of the as-sintered and the carburized materials were acquired using electron probe microanalysis (EPMA 8705QH2) combined WD/ED microanalyzer operated at 20 kV, the line scans were 100 μm wide. Phase identification of the materials was determined by X-ray diffraction (Bruker D8 ADVANCE X-ray diffractometer), Cu Kα radiation, $20° < 2\theta < 110°$ angular range, 0.02° angle step. The microhardness was tested on the cross section of the specimen.

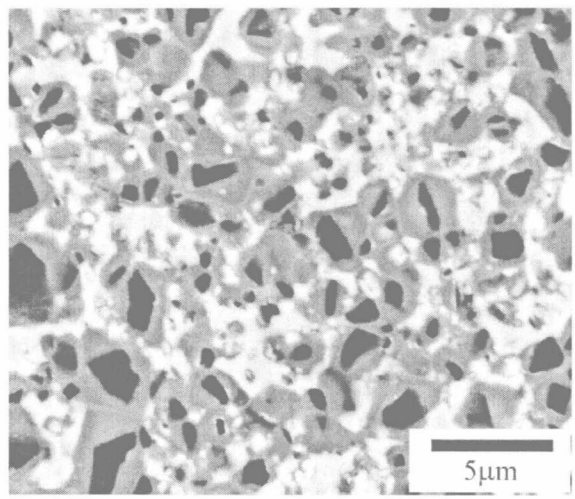

Fig. 2. BSE micrograph of the as-sintered material. The hard phase appears black core-grey rim and white core-grey rim, the binder phase appears white and distributes between the ceramic grains.

3. Results and discussion

3.1. Microstructure

The microstructure of the as-sintered material shows that the carbonitride grains, often with a core-rim structure, are embedded in a tough metallic binder phase, typically in Ti(C, N)-based cermet, as displayed in Fig. 2.

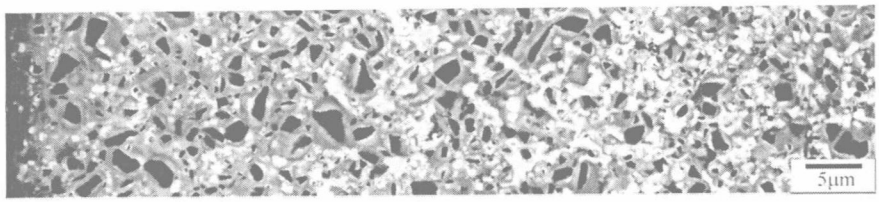

Fig. 3. BSE micrograph of the material carburized at 1200 °C for 180 min. The surface is at the left side.

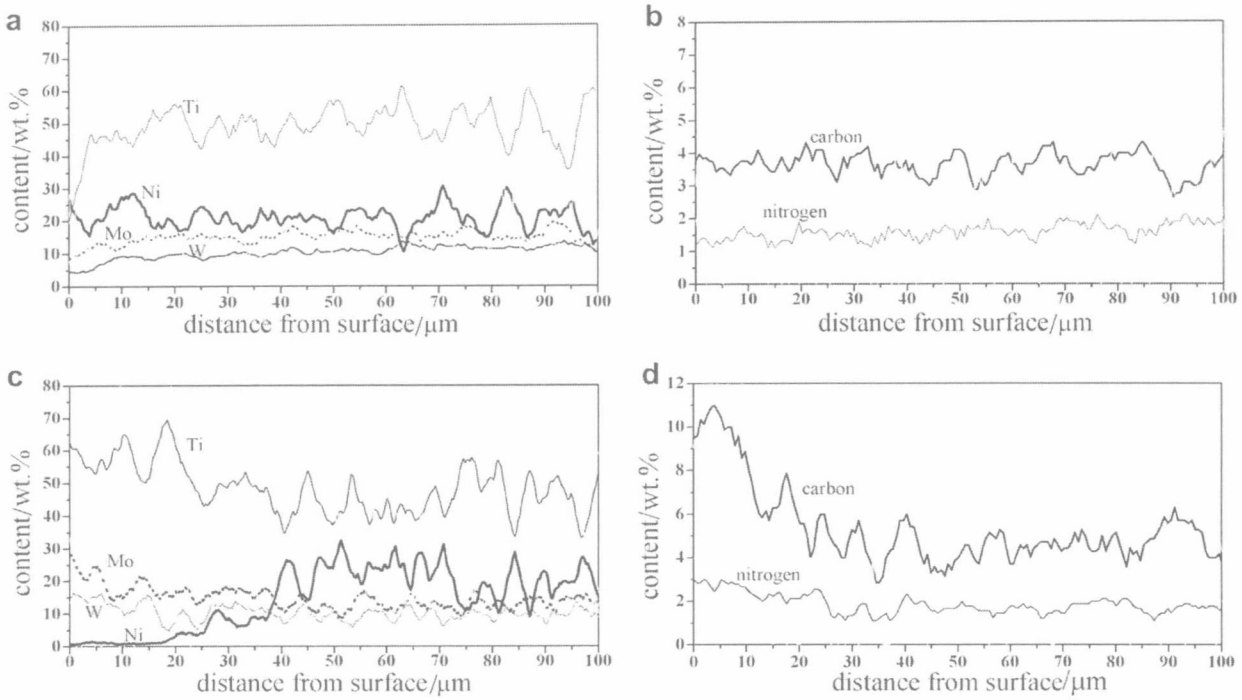

Fig. 4. Compositional line distributions of the as-sintered and carburized: (a, b) as-sintered and (c, d) carburized at 1200 °C for 180 min.

The cores were undissolved Ti(C, N) from the raw powder. The rim, which was introduced by reprecipitation of the carbonitride phases (Ti, Mo, W) (C, N) on the core at different sintering stage, could be divided into inner rim and outer rim. The inner-rim was formed during solid state sintering and enriches in molybdenum and tungsten. The outer rim appearing gray in BSE model was formed during liquid state sintering and contains less molybdenum and tungsten than inner rim [9].

The microstructure of the cermets treated by double-glow plasma carburization at 1200 °C for 180 min is shown in Fig. 3. The binder content decreased abruptly in the surface zone down to about 20 μm depth, then gradually increased inwards, there was a notable increase in the binder content between about 40 μm and 70 μm below the surface. The typical core-rim structure in the surface was reserved after carburization. However the rim became thicker in the area where the binder content was reduced as compared to the as-sintered material.

The EMPA depth profiles are shown in Fig. 4. The results revealed that the elements distributions were constant from surface to bulk in the as-sintered material. After carburization, a notable increase in the contents of carbon, nitrogen, titanium, molybdenum and tungsten was found down to about 40 μm, and the increase ratio in carbon was quite higher than the other elements. The nickel content dropped to near zero in the surface area down to nearly 20 μm, then increased and reached a summit between about 40 μm and 70 μm depth and finally fell to a stable value, which was consistent with distribution of the binder phase.

Since diffusion was substantially faster in the nickel binder than in carbonitride, the binder would act as the main transport medium during carburization. Considering the strong affinity between carbon and titanium, tungsten and molybdenum, reaction occurred as soon as carbon diffused into the nickel binder at high temperature. Here, the reaction could be expressed as follows:

$$C + (Ni.\ Ti.\ Mo,\ W) \rightarrow (Ti,\ Mo.\ W)C + Ni \quad (1)$$

The reaction decreased the concentration of titanium, molybdenum and tungsten in the alloy binder, caused these metallic elements to transport outwards and forced nickel to transfer inwards. The new formed carbides precipitated on original carbonitride grains preferentially, thus, the thickness of the out rim was increased. Since nickel content decreased in the surface area, the binder content was reduced correspondingly. It should also be noted that the relatively high nitrogen content close to the surface resulted from the great decrease in the binder.

3.2. Phase constitution

The XRD patterns of as-sintered and carburized cermets are shown in Fig. 5. Two kinds of phases were observed in the as-sintered samples, the δ phase and γ phase. The δ phase was the carbo-

nitride grains while the γ phase was the binder. Only δ phase was observed at surface of the carburized cermets. Even at 5 μm below the surface, no γ phase was observed. A small quantity of binder was observed at about 23 μm depth. Fig. 6 shows that the (200) diffraction peaks of the δ phase of the carburized cermets at surface and 5 μm below the surface were left-shifted, while it kept almost unchanged at 23 μm depth as compared with the as-sintered material. It is reasonable to estimate that the shift of the δ phase diffraction peaks was caused by the increase of carbon in the carbonitride. As the carbonitride of the as-sintered cermets was always nonstoichiometric because of decarbonization and denitrification during sintering [6], carbon atoms filled the interstitial sites of carbonitride during carburization which could be simply expressed as follows:

$$C + (Ti, W, Mo)(C_x, N_1 - x)_y \rightarrow (Ti, W, Mo)(C_{x'}, N_{1-x'})_{y'} \quad (2)$$

3.3. Performance

The microhardness along the depth is shown in Fig. 7. It was found that the hardness of the surface area was greatly increased by double-glow plasma carburization while the TRS (1816^{+102}_{-122} MPa) was hardly changed, comparing with the as-sintered material (the hardness was 13.550^{+420}_{-380} MPa and the TRS was 1798^{+133}_{-124} MPa).

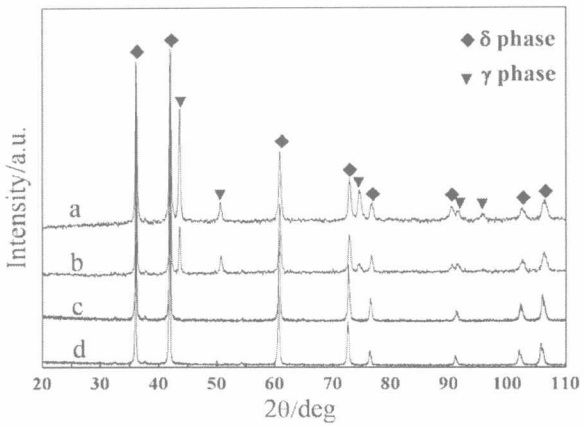

Fig. 5. XRD patterns of (a) as-sintered material, (b) 23 μm below the surface of the carburized material, (c) 5 μm below the surface of the carburized material and (d) the surface of the carburized material.

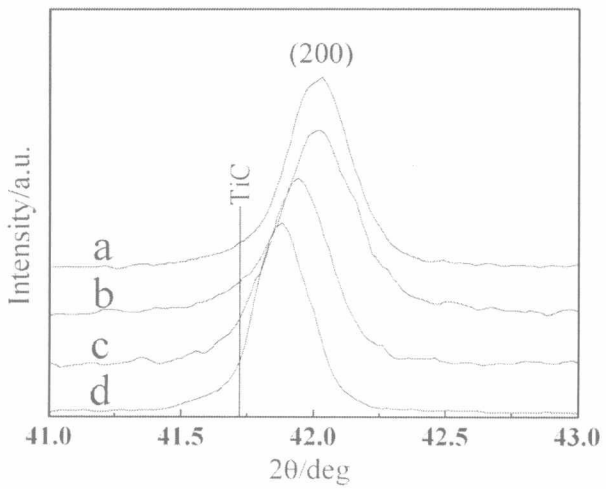

Fig. 6. XRD patterns around the area of the (200) diffraction peaks of (a) as-sintered material, (b) 23 μm below the surface of the carburized material, (c) 5 μm below the surface of the carburized material and (d) the surface of the carburized material.

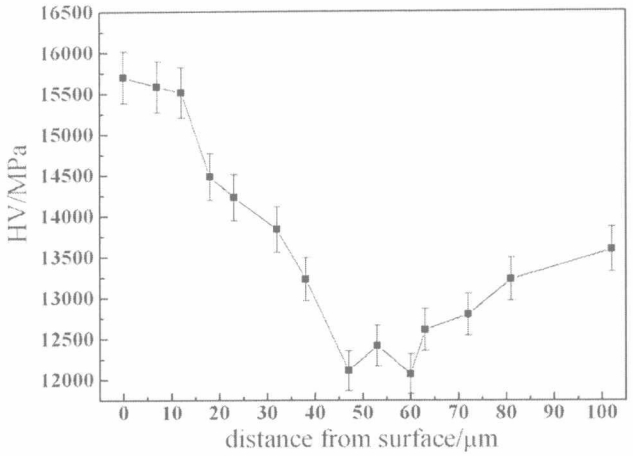

Fig. 7. Hardness distribution on the cross section of the carburized sample.

In general, the surface hardness was increased by inducing a carbonitride-rich layer in the surface zone after carburization. In the meantime, a binder-rich area was formed in the near surface during carburization, which was beneficial to the binding between the surface zone and the substrate.

3.4. Development of the binder-deficient layer

During double-glow plasma carburization, carbon diffused from the surface to interior of cermets, reacted with the metallic elements and drove nickel inwards. As a result, a binder-deficient layer with binder content near zero in the surface zone was formed. Because the binder was nickel-based alloy, it was reasonable to determine the thickness of the binder-deficient layer roughly by measuring the nickel content at different positions of a graded cermet. The experimental results are shown in Fig. 8.

Since the diffusion rate of carbon was much faster than metallic elements, the formation of the binder-deficient layer was mainly controlled by the diffusion of metallic elements and should follow the parabolic law [5]:

$$\text{thickness} \propto \sqrt{\text{time}} \quad (3)$$

Fig. 8a shows that the growth rate of the binder-deficient layer of the cermet with lower nickel content was faster under the same carburization condition, which is in accord with the rule that the formation of the graded layer is controlled by the diffusion of metallic elements. However, the growth of the binder-deficient layer did not follow the parabolic law exactly, it could be ascribed to the great change of diffusion coefficient of the alloy elements under ion bombardment [13].

Vacancy mechanism played the most important role in the substitutional diffusion process. By ion bombardment, supersaturated vacancies were introduced to the material [14], which increased the diffusion probability of the atoms. On the other hand, the diffusion activation energy was reduced in the surface area as the vacancy activation energy could be provided by ion bombardment.

The vacancies annihilated soon when encountered with interstitial atoms, dislocations or grain boundaries during migration, thus, a concentration gradient of vacancy was formed. The diffusion coefficient of the alloy elements changed as a function of vacancy concentration which induced the development of the binder-deficient layer to deviate from the parabolic law. A higher

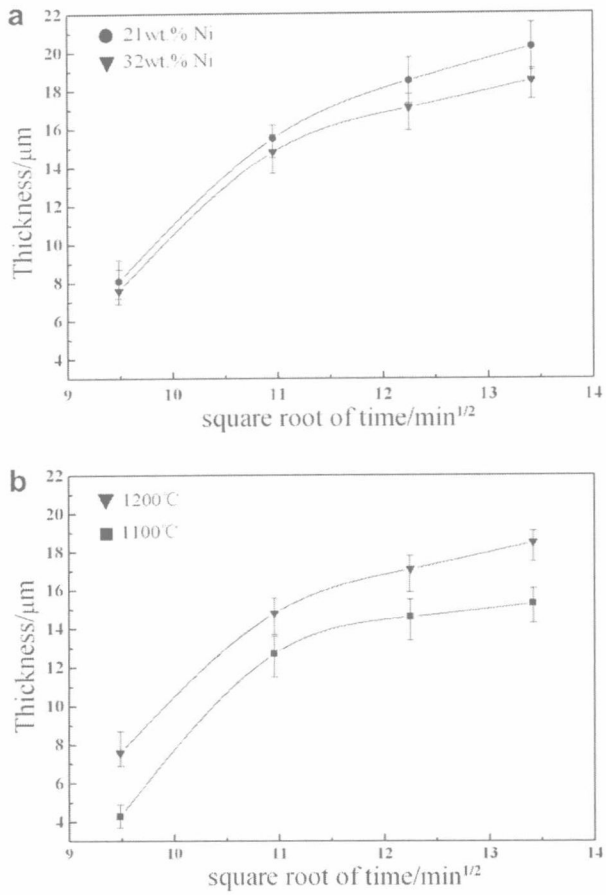

Fig. 8. Thicknesses of the hard phase-rich layer vs square root of time. (a) Materials with different nickel content carburized at 1200 °C; (b) materials with 32 wt.% nickel content carburized at different temperature.

diffusion coefficient was obtained at 1200 °C since the concentration and activity of vacancies were higher at a higher temperature, which is in accord with the result shown in Fig. 8b.

4. Conclusions

(1) A 40 μm surface zone enriched in carbon, titanium, molybdenum, tungsten and nitrogen and deficient in nickel was introduced by double-glow plasma carburization, while the microstructure was influenced down to about 70 μm below the surface.

(2) The differences of affinity between carbon and the metallic elements caused titanium, tungsten and molybdenum to transport towards the surface and nickel inwards during carburization.

(3) The hardness of the surface area was increased after carburization, while the TRS was hardly changed.

(4) The formation of the binder-deficient layer was controlled by the diffusion of the metallic elements but deviates from the parabolic law. Abundant supersaturated vacancies introduced by the ion bombardment enhanced the diffusion coefficient of the elements.

Acknowledgements

This research was financially supported by the National Natural Science Foundation of China under Project No. 50674057, Suzhou Developing Program of Science and Technology under Project No. SG0836.

References

[1] Ettmayer P, Kolaska H, Lengauer W, et al. Ti(C, N) cermets – metallurgy and properties. Int J Refract Met Hard Mater 1995;13:343–51.
[2] Chen L, Lengauer W, Ettmayer P, et al. Fundamentals of liquid phase sintering for modern cermets and functionally graded cemented carbonitrides (FGCC). Int J Refract Met Hard Mater 2000;18(6):307–22.
[3] Lengauer W, Dreyer K. Functionally graded hardmetals. J Alloys Compd 2002;338:1947.
[4] Santhanam AT, Quinto DT. Surface engineering of carbide, cermet and ceramic cutting tools. ASM Handbook, vol. 5. Materials Park, OH: ASM International; 1994.
[5] Suresh S, Mortensen A. Fundamentals of Functionally graded materials, processing and thermomechanical behavior of the graded metals and metal–ceramic composites. Cambridge: IOM Communications Ltd., The University Press Cambridge; 1998.
[6] Ekroth M, Frykholm R, Lindholm M, et al. Gradient zones in WC–Ti(C, N)–Co-based cemented carbides: experimental study and computer simulations. Acta Mater 2000;48:2177–85.
[7] Rosso M, Porto G, Geminiani A. Studies of graded cemented carbides components. Int J Refract Met Hard Mater 1999;17:187–92.
[8] Chen L, Lengauer W, Dreyer K. Advances in modern nitrogen-containing hardmetals and cermets. Int J Refract Met Hard Mater 2000;18:153–61.
[9] Zackrisson J, Rolander U, Weinl G, et al. Microstructure and performance of a cermet material heat-treated in nitrogen. Acta Mater 2000;48:4281–91.
[10] Zhong X, Liu X, Zhang P, et al. Double glow plasma surface alloying and plasma nitriding. Surf Coat Technol 2007;201:4822–5.
[11] Zhong X. A novel plasma surface metallurgy: Xu-Tec process. Surf Coat Technol 1990;43/44:1065–73.
[12] Jiang X, Xishan X, Zhong X. Double glow surface alloying of low carbon steel with electric brush plating Ni interlayer for improvement in corrosion resistance. Surf Coat Technol 2003;168:156–60.
[13] Metin E, Inal OT. Formation and growth of iron nitrides during ion-nitriding. J Mater Sci 1987;22:2783–8.
[14] Zhonghou L, Yongan S. Determination of diffusivity on tungsten and molybdenum in double glow discharge. J Acta Mater 1995;8(2):145.